Structural Comparison of Apomyoglobin and Metaquomyoglobin: pH Titration of Histidines by NMR Spectroscopy†

Melanie J. Cocco,‡ Yung-Hsiang Kao,‡ Allen T. Phillips,§ and Juliette T. J. Lecomte*,‡
Department of Chemistry and Department of Biochemistry, The Pennsylvania State University, University Park, Pennsylvania 16802

Received February 20, 1992; Revised Manuscript Received April 28, 1992

ABSTRACT: Proton NMR spectroscopy was applied to myoglobin in the ferric, water-liganded form (metMbH_2O) and the apo form (apoMb) to probe the structure and stability of the latter. Proteins from sperm whale and horse skeletal muscles were studied to simplify the spectral assignment task. Nuclear Overhauser effects and the response of chemical shifts to variations of pH were used as indicators of residual native holoprotein structure in the apoprotein. The investigation was focused on the histidine side chains and their environment. In metMbH_2O, the resonances of all imidazole rings not interacting with the heme were assigned by applying standard two-dimensional methods. These assignments were found to differ from those reported elsewhere [Carver, J. A., & Bradbury, J. H. (1984) *Biochemistry 23*, 4890–4905] except for His-12, -113, and -116. Only one histidine (His-36) has a pK_a higher than 7, two (His-48 and His-113) have a pK_a lower than 5.5, and two (His-24 and His-82) appear not to titrate between pH 5.5 and pH 10. In the apoproteins, the signals of His-113 and His-116, as well as those of His-24, -36, -48, and -119 previously assigned in the horse globin [Cocco, M. J., & Lecomte, J. T. J. (1990) *Biochemistry 29*, 11067–11072], could be followed between pH 5 and pH 10. A comparison to the holoprotein data indicated that heme removal has limited effect on the pK_a and the surroundings of these residues. Five additional histidines which occur in the two helices and connecting loops forming the heme binding site were identified in the horse apoprotein. Four of these were found to have pK_a values lower than that expected of an exposed residue. The NOE and titration data were proposed to reflect the fact that several holoprotein structural elements, in particular outside the heme binding site, are maintained in the apoprotein. In the heme binding region of the apoprotein structure, the low pK_a's suggest local environments which are resistant to protonation.

The folding of small water-soluble globular proteins generally proceeds rapidly under native conditions (Levinthal, 1968). The process is strongly cooperative, and in most cases, there is no stable, populated intermediate between the fully unfolded form and the native form (Baldwin, 1975; Kim & Baldwin, 1982). Intermediates are a potential source of information on this complex conformational transition, and their absence has limited the understanding of how the forces stabilizing the native structure develop during folding.

One approach toward evaluating the determinants of structure and stability is to examine the apo form of proteins which normally contain a strongly interacting prosthetic group. Removal of this group from the polypeptide matrix results in destabilization and, often, in structural changes (Anfinsen & Sheraga, 1975). If, in the latter case, the native holoprotein can be obtained quantitatively from the apoprotein by simple addition of the prosthetic group in vitro, the apoprotein can be considered as a precursor to the native form and perhaps the product of an arrested folding reaction. The study of its structural and thermodynamic properties under native conditions offers an otherwise inaccessible description of the preponderant interactions in a possible folding intermediate. Such strategy has been applied to apocytochrome b_5 (Moore & Lecomte, 1990; Moore et al., 1991; Lecomte & Moore, 1991), apocytochrome b_{562} (Feng et al., 1991; Feng & Sligar, 1991), and apomyoglobin (Cocco & Lecomte, 1990).

Myoglobin (Mb)[1] is a globular, α-helical *b* heme protein of moderate size ($M_r \approx 17\,900$; 153 residues). Its structure (Takano, 1977) is depicted in Figure 1. Myoglobin is a good candidate for the study of partially folded species because the removal of its heme is known to lower its secondary structure content (Breslow et al., 1965; Harrison & Blout, 1965), decrease its stability (Griko et al., 1988), and enhance the backbone dynamics (Abrash, 1970; Hughson et al., 1990). Interest in the apoprotein of myoglobin (referred to as apomyoglobin or globin in this work) has grown in the last few years, in particular since the discovery of a stable intermediate form at acidic pH (Irace et al., 1986; Griko et al., 1988), the detection of a cold-denaturation transition (Griko et al., 1988), and the observation that apoMb behaves as a molten globule at pH lower than 5 when the ionic strength is adequately adjusted (Goto & Fink, 1990; Goto et al., 1990). ApoMb has thus become a challenging protein for the theoretical modeling of protein stability and dynamics (Chan & Dill, 1991; Stigter et al., 1991; Brooks, 1992).

Under native conditions, apoMb contains some degree of residual holoprotein structure (Anderson et al., 1970; Griko et al., 1988). This is apparent in NMR data: at least four

* To whom correspondence should be addressed: Department of Chemistry, The Pennsylvania State University, University Park, PA 16802.

† This work was supported in part by the donors of the Petroleum Research Fund, administered by the American Chemical Society.

‡ Department of Chemistry.
§ Department of Biochemistry.

[1] Abbreviations: apoMb, apomyoglobin, globin; CD, circular dichroism; des-Fe Mb, protoporphyrin IX–globin complex; DIPSI, decoupling in the presence of scalar interactions; DQF-COSY, two-dimensional double-quantum-filtered correlated spectroscopy; DSS, sodium 2,2-dimethyl-2-silapentane-5-sulfonate; holoMb, holomyoglobin; Mb, myoglobin; MbCO, carbonmonoxymyoglobin; metMb, ferrimyoglobin; metMbH_2O, metMb^2H_2O, metaquomyoglobin; metMbOH, methydroxymyoglobin; NMR, nuclear magnetic resonance; NOE, nuclear Overhauser effect; NOESY, two-dimensional nuclear Overhauser spectroscopy; TOCSY, total correlation spectroscopy; TPPI, time proportional phase incrementation; 2Q, two-quantum spectroscopy.

0006-2960/92/0431-6481$03.00/0

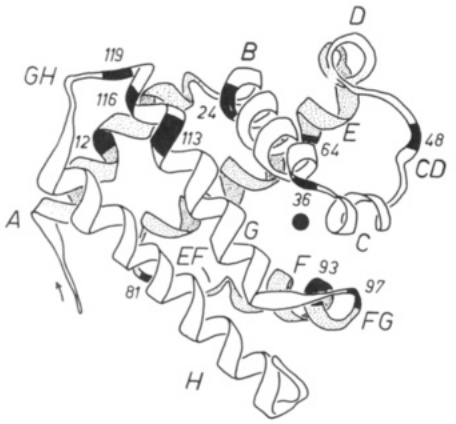

FIGURE 1: The fold of myoglobin [after Takano (1977)]. Helices are labeled with a single letter and connecting turns with two letters. Histidine α-carbons are indicated by a blackened stretch of ribbon. Histidines are found at the following positions: 12 (A10, present only in sperm whale myoglobin), 24 (B5), 36 (C1), 48 (CD6), 64 (E7, distal), 81 (EF4), 82 (EF5, hidden behind the H helix and not numbered), 93 (F8, proximal), 97 (FG3), 113 (G14), 116 (G17), and 119 (GH1). The filled circle marks the location of the heme iron atom.

clusters of residues can be recognized which survive heme extraction (Cocco & Lecomte, 1990). These clusters are composed mostly of hydrophobic residues and indicate that tertiary interactions occur in two distinct regions of the protein, one which involves residues from the CD corner and the adjacent C and D helices as well as the G helix, and another containing elements of the A, B, G, and H helices. Equilibrium unfolding studies have implicated the stabilizing contributions of specific residues within the BG interface of human apoMb (Hughson & Baldwin, 1989) and the AH and GH interfaces of sperm whale apoMb (Hughson et al., 1991), lending support to the hypothesis that these interfaces play a role in the determination of the native apoprotein fold.

As a consequence of the partial unfolding, it has proven difficult to interpret the NMR spectra of apoMb and to describe the spatial arrangement of the backbone and most side chains. Our previous efforts (Cocco & Lecomte, 1990) focused on the presence of hydrophobic clusters. Conclusions were based on a limited number of nuclear Overhauser connectivities and provided a preliminary survey of structural features. To characterize the apoprotein fold further, we now resort to a combination of nuclear Overhauser effects and response of the spectrum to variations of pH. As additional structural reporters, we use histidine residues.

Histidines give rise to characteristic ring resonances, generally sharper than other signals, which can often be recognized in the proton spectrum of a partially unfolded species. These resonances are remarkably sensitive to the electrostatic and structural properties of the environment (Markley, 1975). Thus, we monitored the titration behavior of all resolved imidazole ring signals in the apoprotein of myoglobin. The histidines contained in the clusters mentioned above provide direct insight into the structural integrity and stability of the native apoprotein fold. In addition, it is possible to determine the pK_a of the imidazole side chains which reside in the heme binding site. This site is created by the E–EF–F–FG elements, where assignments and structural information are not yet available. To interpret our results we engaged in a comparative study of ferrimyoglobin.

The denaturation of apomyoglobin at low pH is accompanied by swelling of the molecule and the protonation of buried imidazole groups (Katz et al., 1973; Irace et al., 1986). The modeling of electrostatic and hydrophobic interactions confirms that preventing ionization by burying histidines destabilizes the folded apoprotein at low pH (Stigter et al., 1991). The response of the NMR spectrum to pH, combined with the pK_a data, allows us to identify those residues which play a unique role in the structure and elucidate their state of protonation at low pH.

Materials and Methods

Protein Samples. Horse Mb (Sigma type IV) and sperm whale Mb (Sigma) were used without further purification. For pH titrations of metMb, the protein was dissolved into ^2H_2O for 24–36 h and then lyophilized; this was repeated two to three times. Final concentrations were approximately 3 mM in protein. MetMb samples for 2D NMR experiments in ^2H_2O were reconstituted from apoMb, which was prepared and exchanged as described previously (Cocco & Lecomte, 1990). Hemin (Sigma) was dissolved in 0.01 M NaO^2H and 1.5–2 equiv was added to the apoMb solution. The sample was then spun in an Eppendorf centrifuge to remove precipitate and concentrated to between 3 and 4 mM with an Amicon Centricon-10 microconcentrator (YM10 membrane). The pH* (uncorrected meter reading) was adjusted to 5.7 with 0.1 M ^2HCl. ApoMb samples for pH titrations and 2D NMR experiments were exchanged into ^2H_2O by using solubilization and lyophilization; final protein concentrations were between 1 and 2 mM.

NMR Experiments. One- and two-dimensional proton NMR spectra were acquired as previously described on a Bruker AM-500 spectrometer at 298 K (Lecomte & Cocco, 1990). A spectral width of 6024 Hz and 16 192 data points were used to acquire one-dimensional pH titration spectra. These were zero-filled up to 32 384 points and resolution-enhanced by using a sine-bell function with a shift between 0° and 45°. 2D NMR experiments were recorded in the phase-sensitive mode with the TPPI method (Drobny et al., 1979; Marion & Wüthrich, 1983) and included DQF-COSY (Rance et al., 1983), 2Q (Braunschweiler et al., 1983; Rance & Wright, 1986), TOCSY (Braunshweiler & Ernst, 1983; Rance, 1987), and Hahn-echo NOESY (Kumar et al., 1980; Bodenhausen et al., 1984; Davis, 1989). 2Q data were acquired with 64 transients for each t_1 value; mixing times were 40 and 80 ms. Spin-locking in TOCSY experiments was performed by using the DIPSI-2 sequence of Shaka et al. (1988), which was repeated to achieve a 70-ms mixing time. Hahn-echo NOESY mixing times were 110 ($metMbH_2O$) and 100 ms (apoMb). A total of 64 or 96 transients were collected for each of the 460–512 t_1 values. Both TOCSY and NOESY experiments were sine-modulated in the t_1 domain (Otting et al., 1986). Two-dimensional data were processed as previously described (Lecomte & Cocco, 1990).

$MetMbH_2O$ spectra were recorded at 298 K with the same parameters as for a diamagnetic protein. Data sets were also collected at 308 K to resolve spectral overlap and to identify protons resonating within the diamagnetic spectral width which are under the influence of the paramagnetic center. Chemical shifts are referenced to DSS through residual H_2O at 4.76 (298 K) and 4.65 ppm (308 K).

pH Titrations. A protein solution of 0.8–1.0 mL at pH ca. 7 was divided into two equal volume samples; one for use in titrating to the acidic region, the other to the basic region. The pH* of the solution was adjusted with 0.1 M NaO^2H or ^2HCl to record spectra every 0.2–0.3 pH unit. A Beckman ϕ71 pH meter equipped with an Ingold combination electrode (6030-1M) was used for pH measurements. The pH of the solutions was determined before and after each NMR data collection. Excellent agreement between the two readings was observed

Table I: Chemical Shifts of Selected Resonances in Metaquomyoglobin[a]

Leu-2	eq	$C^{\beta}Hs$, 0.59, 1.11; $C^{\gamma}H$, 1.20; $C^{\delta 1}H_3$, 0.38; $C^{\delta 2}H_3$, −0.30
	sw	$C^{\gamma}H$, 1.19; $C^{\delta 1}H_3$, 0.46; $C^{\delta 2}H_3$, −0.31
Trp-7	eq	$C^{\delta}H$, 7.11; $N^{\epsilon}H$, 9.78; $C^{\zeta 2}H$, 7.23; $C^{\eta}H$, 7.43; $C^{\zeta 3}H$, 7.23; $C^{\epsilon 3}H$, 7.57
	sw	$C^{\delta}H$, 7.01; $N^{\epsilon}H$, 9.81; $C^{\zeta 2}H$, 7.23; $C^{\eta}H$, 7.44; $C^{\zeta 3}H$, 7.23; $C^{\epsilon 3}H$, 7.54
His-12	sw	$C^{\delta}H$, 7.29; $C^{\epsilon}H$, 8.44
Val-13	eq	$C^{\alpha}H$, 3.72; $C^{\beta}H$, 2.48; $C^{\gamma 1}H_3$, 1.04; $C^{\gamma 2}H_3$, 1.19
	sw	$C^{\alpha}H$, 3.67; $C^{\beta}H$, 2.50; $C^{\gamma 1}H_3$, 1.05; $C^{\gamma 2}H_3$, 1.19
Trp-14	eq	$C^{\delta}H$, 7.19; $N^{\epsilon}H$, 10.47; $C^{\zeta 2}H$, 7.85; $C^{\eta}H$, 7.20; $C^{\zeta 3}H$, 6.91; $C^{\epsilon 3}H$, 7.31
	sw	$C^{\delta}H$, 7.15; $N^{\epsilon}H$, 10.47; $C^{\zeta 2}H$, 7.77; $C^{\eta}H$, 7.15; $C^{\zeta 3}H$, 6.89; $C^{\epsilon 3}H$, 7.28
Val-17	eq	$C^{\alpha}H$, 1.65; $C^{\beta}H$, 0.90; $C^{\gamma 1}H_3$, −0.02; $C^{\gamma 2}H_3$, −0.51
	sw	$C^{\alpha}H$, 1.44; $C^{\beta}H$, 0.90; $C^{\gamma 1}H_3$, −0.13; $C^{\gamma 2}H_3$, −0.53
His-24	eq	$C^{\delta}H$, 6.14; $C^{\epsilon}H$, 7.87
	sw	$C^{\delta}H$, 6.14; $C^{\epsilon}H$, 7.79
His-36	eq	$C^{\delta}H$, 7.35; $C^{\epsilon}H$, 8.21
	sw	$C^{\delta}H$, 7.33; $C^{\epsilon}H$, 8.30
Phe-46	eq	$C^{\alpha}H$, 4.80
	sw	$C^{\alpha}H$, 4.81
His-48	eq	$C^{\delta}H$, 6.99; $C^{\epsilon}H$, 8.04
	sw	$C^{\delta}H$, 7.02; $C^{\epsilon}H$, 8.09
Leu-49	eq	$C^{\gamma}H$, 0.74; $C^{\delta 1}H_3$, 0.32; $C^{\delta 2}H_3$, 0.32
	sw	$C^{\gamma}H$, 0.78; $C^{\delta 1}H_3$, 0.36; $C^{\delta 2}H_3$, 0.36
Leu-76	eq	$C^{\gamma}H$, 1.89; $C^{\delta 1}H_3$, 0.20; $C^{\delta 2}H_3$, 1.09
	sw	$C^{\gamma}H$, 1.91; $C^{\delta 1}H_3$, 0.14; $C^{\delta 2}H_3$, 1.10
His-81	eq	$C^{\beta}Hs$, 3.10, 3.35; $C^{\delta}H$, 7.12; $C^{\epsilon}H$, 8.42
	sw	$C^{\beta}Hs$, 3.11, 3.37; $C^{\delta}H$, 7.13; $C^{\epsilon}H$, 8.46
His-82	eq	$C^{\alpha}H$, 5.38; $C^{\delta}H$, 6.64; $C^{\epsilon}H$, 7.67
	sw	$C^{\alpha}H$, 5.37; $C^{\delta}H$, 6.63; $C^{\epsilon}H$, 7.71
Leu-86	eq	$C^{\beta}Hs$, 1.23, 1.38; $C^{\gamma}H$, 1.09; $C^{\delta 1}H_3$, 0.29; $C^{\delta 2}H_3$, 0.38
	sw	$C^{\gamma}H$, 1.14; $C^{\delta 1}H_3$, 0.28; $C^{\delta 2}H_3$, 0.34
Tyr-103	eq	$C^{\delta/\epsilon}H$, 8.53; $C^{\epsilon/\delta}H$, 7.95
	sw	$C^{\delta/\epsilon}H$, 8.56; $C^{\epsilon/\delta}H$, 7.97
Phe-106	eq	$C^{\delta}H$, 7.39; $C^{\epsilon}H$, 7.78; $C^{\zeta}H$, 7.73
	sw	$C^{\delta}H$, 7.31; $C^{\epsilon}H$, 7.77; $C^{\zeta}H$, 7.70
His-113	eq	$C^{\delta}H$, 6.82; $C^{\epsilon}H$, 7.97
	sw	$C^{\delta}H$, 6.67; $C^{\epsilon}H$, 7.77
Val-114	eq	$C^{\alpha}H$, 3.45; $C^{\beta}H$, 1.89; $C^{\gamma 1}H_3$, 0.77; $C^{\gamma 2}H_3$, 0.56
	sw	$C^{\alpha}H$, 3.49; $C^{\beta}H$, 1.85; $C^{\gamma 1}H_3$, 0.76; $C^{\gamma 2}H_3$, 0.69
Leu-115	eq	$C^{\gamma}H$, 1.74; $C^{\delta 1}H_3$, 0.56; $C^{\delta 2}H_3$, 0.77
	sw	$C^{\gamma}H$, 1.74; $C^{\delta 1}H_3$, 0.51; $C^{\delta 2}H_3$, 0.73
His-116	eq	$C^{\delta}H$, 7.40; $C^{\epsilon}H$, 8.37
	sw	$C^{\delta}H$, 7.44; $C^{\epsilon}H$, 8.40
His-119	eq	$C^{\delta}H$, 6.85; $C^{\epsilon}H$, 8.40
	sw	$C^{\delta}H$, 6.78; $C^{\epsilon}H$, 8.39
Phe-123	eq	$C^{\delta}H$, 7.19; $C^{\epsilon}H$, 7.32; $C^{\zeta}H$, 7.13
	sw	$C^{\delta}H$, 7.21; $C^{\epsilon}H$, 7.39; $C^{\zeta}H$, 7.17
Met-131	eq	$C^{\epsilon}H_3$, 2.43
	sw	$C^{\epsilon}H_3$, 2.42
Phe-151	eq	$C^{\delta}H$, 5.84; $C^{\epsilon}H$, 6.34; $C^{\zeta}H$, 6.16
Tyr-151	sw	$C^{\delta/\epsilon}H$, 5.66; $C^{\epsilon/\delta}H$, 5.80

[a] Chemical shifts at pH* 5.7 (pH 5.7 for exchangeable protons) and 298 K are reported in ppm with respect to the water line at 4.76 ppm; eq refers to horse metMbH_2O; sw refers to sperm whale metMbH_2O. The denomination "1" and "2" for methyl groups of valines and leucines is chosen according to holoprotein solid-state structure predictions (Takano, 1977; Evans & Brayer, 1990).

for the apoproteins, whereas for the holoproteins, values occasionally deviated (within 0.06 pH unit at most). In those cases the second measurement was considered more accurate. Our titration curves were reproduced at least twice; the results were independent of the electrodes used. All pH readings in ^2H_2O are reported as pH*. The increase in ionic strength throughout the titration was limited to 0.02 M.

Titration Data Fitting. The chemical shift of histidine $C^{\delta}H$ and $C^{\epsilon}H$ resonances as a function of pH was fitted to the following equation with a nonlinear least-squares fitting procedure

$$\delta_i = \delta_{His} + (\delta_{His^+} - \delta_{His})\{10^{n(pK-pH)}/[1 + 10^{n(pK-pH)}]\}$$

This Henderson–Hasselbalch equation applies when the protonation–deprotonation process is fast on the NMR time scale (Markley, 1975); the chemical shift at any pH, δ_i, is then a weighted average of the imidazole chemical shift, $\delta_{(His)}$, and the imidazolium chemical shift, δ_{His^+}. The Hill coefficient (n), δ_{His}, δ_{His^+}, and the apparent pK_a are adjustable parameters. MetMb undergoes hemic acid dissociation at basic pH, and resulting spectral perturbations are observed above pH 8.5. Thus, only data points with pH <8.5 were used in the holoprotein fits. Data listed in Tables III and IV include the standard deviation on n and pK_a to illustrate the quality of the fit. For a well-defined titration curve, the pK_a value is thought to be accurate within an error of ±0.1 pH unit (even when standard deviation of the fit and estimated uncertainty are much lower). The error increases when only a partial curve is obtainable, and in extreme cases, we limit the interpretation to an upper limit to the pK_a value.

Centrifugation. Sedimentation equilibrium studies were performed in a Spinco Model E analytical ultracentrifuge equipped with a photoelectric scanner, multiplexer, and variable-wavelength light source. Experiments were conducted at 20 °C and 30000 rpm in an AnF-Ti four-place rotor. Samples were prepared in water and adjusted to pH 6.0 with NaOH. These were then analyzed in cells fitted with sapphire windows and charcoal-filled Epon double-sector centerpieces of 12-mm thickness; sample volume was 0.2 mL, and water was used in the reference sector. Absorbance data were collected at either 310 or 315 nm after approximately 60 h of centrifugation. At these wavelengths, concentration distributions ranging from 0.01 to 1.0 mM could be reliably monitored.

Results

Assignment of Histidine $C^{\delta}H$ and $C^{\epsilon}H$ in MetMbH_2O. The most recent systematic study of histidine resonances in sperm whale and horse metMbH_2O was reported several years ago by Carver and Bradbury (1984). To assign the signals to specific residues, these authors used the results of Botelho and Gurd (1978) and applied three methods: (1) comparison of the one-dimensional spectra of Mbs from different species, (2) inspection of the one-dimensional spectra after chemical modification of the histidine residues, and (3) pairing of pK_a values obtained from $C^{\delta}H$ and $C^{\epsilon}H$. As indicated by Dalvit and Wright (1987), these assignments need to be reexamined and we applied 2D techniques to this end. In order to locate the signals of His-24, -36, -48, and -119 found in both horse and sperm whale metMbH_2O, we searched for the NOE patterns observed in sperm whale MbCO (Dalvit & Wright, 1987), horse MbCO (Lecomte & Cocco, 1990), and the structurally similar des-Fe Mbs (Lecomte & Cocco, 1990). In addition, we assigned His-12 (A10) (present in sperm whale Mb only), -81 (EF4), -82 (EF5), -113 (G14), and -116 (G17) on the basis of dipolar contacts: His-12 to Val-13, His-82 to Leu-86, His-113 to Val-114, and His-116 to Phe-123. His-81 (EF4) was assigned through a backbone NOE connectivity to His-82. The remaining three histidines, His-64 (E7, distal), -93 (F8, proximal), and -97 (FG3), are close to the heme iron, with $C^{\delta}H$ and $C^{\epsilon}H$ at distances shorter than 7.5 Å, and are not observed under our conditions. The NOE connectivities are qualitatively consistent with the solid-state structure of sperm whale metMbH_2O (Takano, 1977) and horse metMbH_2O (Evans & Brayer, 1990). Details of the assignment process are provided in the supplementary material and chemical shifts are listed in Table I.

Assignment of Histidine $C^{\delta}H$ and $C^{\epsilon}H$ in ApoMb. We recently determined that horse apoMb retains structural features of the holoprotein observable by 2D ^1H NMR techniques (Cocco & Lecomte, 1990). Key to that work was the assignment of signals from the two tryptophans (Trp-7 and

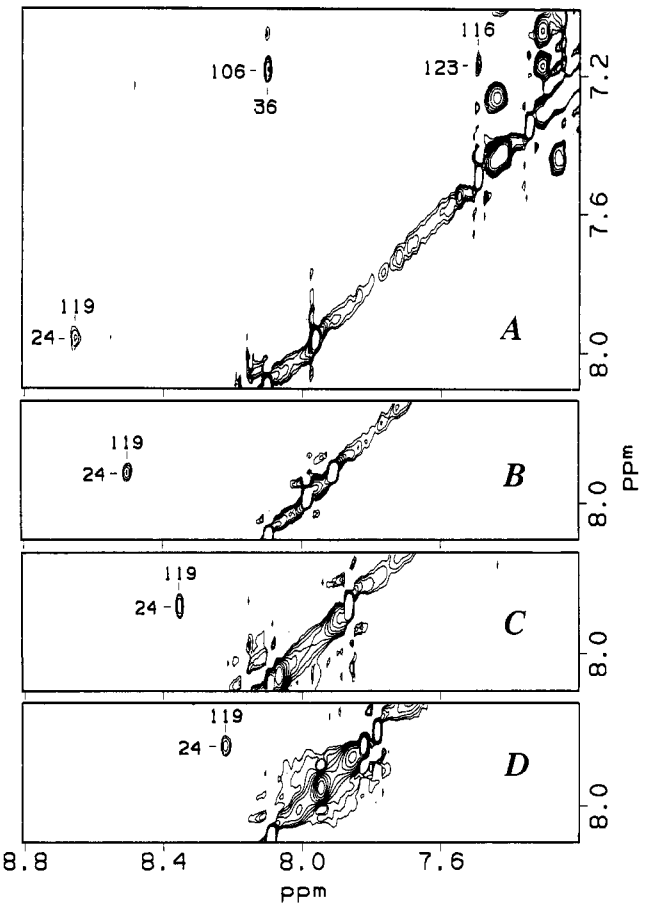

FIGURE 2: Phase-sensitive NOESY spectra of a 2 mM sample of sperm whale apoMb recorded at 500 MHz in ^2H_2O at 298 K at different pH* values with a mixing time of 100 ms. (A) Portion of the aromatic region at pH* 5.2. His-116 is assigned through its dipolar contact with Phe-123. Note the NOE between His-24 $C^\epsilon H$ and His-119 $C^\epsilon H$. This same NOE is found at (B) pH* 5.5, (C) pH* 5.7, and (D) pH* 6.1. The figure demonstrates the ability to follow signals and verify structural integrity throughout the titration by monitoring specific cross peaks.

Trp-14), the two methionines (Met-55 and Met-131), and one of the two tyrosines (Tyr-103). Overall, the assigned residues cluster in four groups, each maintaining a conformation similar to that in the holoprotein; His-24, -36, -48, and -119 are located within these four groups. The NMR experiments performed on horse apoMb were carried out on sperm whale apoMb and allowed for the same sets of residues to be recognized in this protein. In spite of occasional frequency shifts, the NOE patterns are comparable and the spectra used for assignment purposes are not shown here.

It is also possible to identify other histidines (the remaining seven in horse Mb and five of the remaining eight in sperm whale Mb) by analyzing TOCSY and 2Q spectra. For example, in horse apoMb His-24 has a weak NOE to a methyl group which, according to its TOCSY connectivities, belongs to a valine residue. This methyl group has a strong NOE to the $C^\delta H$ of another histidine. Comparison to the holoprotein data points to Val-114 and the assignment to His-113. Figure 2A presents a limited section of the aromatic region of a sperm whale apoMb NOESY spectrum. In addition to the 36 ↔ 106 and 24 ↔ 119 connectivities previously reported for the horse protein [Figure 4 in Cocco and Lecomte (1990)], it shows a NOE between Phe-123 and a histidine residue recognized here as His-116. The other histidine residues could not be assigned unambiguously, and in the rest of this work, we label them as H-1-eq through H-5-eq in horse apoMb and H-1-sw through H-3-sw in sperm whale apoMb. The labels are chosen sequentially from lowest field to highest field for the $C^\epsilon H$ signal at pH* 5.7, and we caution that residue H-*n*-eq may not necessarily correspond to residue H-*n*-sw. Chemical shifts of histidine $C^\delta H$ and $C^\epsilon H$ and other protons important to the assignment process are listed in Table II.

Table II: Chemical Shifts of Selected Resonances in Apomyoglobin[a]

Leu-2	$C^\beta H$, 0.69; $C^\gamma H$, 1.11; $C^{\delta 1}H_3$, 0.24; $C^{\delta 2}H_3$, −0.33
Trp-7	$C^\delta H$, 6.92; $N^\epsilon H$, 9.86; $C^{\zeta 2}H$, 7.22; $C^\eta H$, 6.96; $C^{\zeta 3}H$, 7.44
Trp-14	$C^\delta H$, 6.94; $N^\epsilon H$, 10.23; $C^{\zeta 2}H$, 7.41; $C^\eta H$, 6.92; $C^{\zeta 3}H$, 6.64; $C^{\epsilon 3}H$, 7.03
Val-17	$C^\alpha H$, 1.62; $C^\beta H$, 0.83; $C^{\gamma 1}H_3$, −0.38; $C^{\gamma 2}H_3$, 0.02
His-24	$C^\delta H$, 6.35; $C^\epsilon H$, 7.87
Phe-33	$C^\delta H$, 7.06; $C^\epsilon H$, 6.79; $C^\zeta H$, 6.44
His-36	$C^\delta H$, 7.06; $C^\epsilon H$, 8.06
Leu-40	$C^\beta H$, 1.62; $C^{\beta'} H$, 1.34; $C^\gamma H$, 1.26; $C^{\delta 1}H_3$, 0.28; $C^{\delta 2}H_3$, 0.40
Phe-43	$C^\delta H$, 7.38; $C^\epsilon H$, 7.25; $C^\zeta H$, 7.00
Phe-46	$C^\alpha H$, 5.02; $C^\delta H$, 6.92; $C^\epsilon H$, 6.85; $C^\zeta H$, 6.79
His-48	$C^\delta H$, 7.07; $C^\epsilon H$, 8.12
Leu-49	$C^\gamma H$, 1.12; $C^{\delta 1}H_3$, 0.70; $C^{\delta 2}H_3$, 1.00
Met-55	$C^\epsilon H_3$, 1.84
Leu-76	sw $C^\gamma H$, 1.41; $C^{\delta 1}H_3$, −0.21; $C^{\delta 2}H_3$, 0.62
	eq $C^\gamma H$, 1.37; $C^{\delta 1}H_3$, −0.06; $C^{\delta 2}H_3$, 0.58
Tyr-103	$C^{\delta/\epsilon}H$, 6.87; $C^{\epsilon/\delta}H$, 6.95
Phe-106	$C^\delta H$, 6.70; $C^{\epsilon\zeta}H$, 7.18
His-113	sw $C^\delta H$, 6.79; $C^\epsilon H$, 7.82
	eq $C^\delta H$, 6.98; $C^\epsilon H$, 8.14
Val-114	sw $C^\alpha H$, 3.63; $C^\beta H$, 2.06; $C^{\gamma 1}H_3$, 0.98; $C^{\gamma 2}H_3$, 1.08
	eq $C^\alpha H$, 3.65; $C^\beta H$, 2.09; $C^{\gamma 1}H_3$, 0.85; $C^{\gamma 2}H_3$, 1.08
Leu-115	$C^\beta H$, 0.10; $C^{\beta'} H$, 1.24; $C^\gamma H$, 1.76; $C^{\delta 1}H_3$, 0.52; $C^{\delta 2}H_3$, 0.61
His-116	sw $C^\delta H$, 7.41; $C^\epsilon H$, 8.33
	eq $C^\delta H$, 7.41; $C^\epsilon H$, 8.43
His-119	$C^\delta H$, 6.69; $C^\epsilon H$, 8.31
Phe-123	$C^\delta H$, 7.16; $C^\epsilon H$, 7.31; $C^\zeta H$, 7.06
Met-131	$C^\epsilon H_3$, 2.14
H-1-sw	$C^\delta H$, 7.25; $C^\epsilon H$, 8.37
H-2-sw	$C^\delta H$, 7.07; $C^\epsilon H$, 8.32
H-3-sw	$C^\delta H$, 6.97; $C^\epsilon H$, 7.97
H-1-eq	$C^\delta H$, 7.04; $C^\epsilon H$, 8.30
H-2-eq	$C^\delta H$, 7.08; $C^\epsilon H$, 8.26
H-3-eq	$C^\delta H$, 7.14; $C^\epsilon H$, 8.17
H-4-eq	$C^\delta H$, 7.02; $C^\epsilon H$, 8.04
H-5-eq	$C^\delta H$, 6.68; $C^\epsilon H$, 7.86

[a] Sperm whale (sw) apomyoglobin chemical shifts at pH* 5.7 (pH 5.7 for exchangeable protons) and 298 K are reported in ppm with respect to the water line at 4.76 ppm. Horse apomyoglobin chemical shifts can be found in Cocco and Lecomte (1990). Additional horse apoMb chemical shifts are listed with "eq" qualifying the residue. The denomination "1" and "2" for methyl groups of valines and leucines is chosen according to holoprotein solid-state structure predictions (Takano, 1977; Evans & Brayer, 1990).

Sedimentation equilibrium experiments performed on horse, sperm whale (Crumpton et al., 1965), and seal I (Rumen & Apella, 1962) apoMbs have indicated that these proteins remain monomeric at concentrations up to 0.5 mM at pH 7.7. Aggregate formation was demonstrated at low pH for seal I apoMb. To ensure that a similar association of horse or sperm whale apoMb does not occur near neutral pH at the concentration used for our initial spectral assignments, we carried out sedimentation experiments extending the concentration range to 1 mM, the lower concentration limit for our NMR studies. Data from the sedimentation equilibrium studies gave linear plots of ln (concentration) versus (distance)[2] throughout the concentration range examined, and no evidence for forms larger than the monomeric species was obtained. Analysis at 10000 rpm to detect large aggregated species that might sediment extensively at the normal equilibrium speed chosen (30000 rpm) revealed that no significant amount of such material was present. However, at pH values lower than 5,

[2] The difference in reactivity toward bromoacetate reported for this residue in the apoprotein and holoprotein forms of Mb (Banaszak et al., 1963; Breslow, 1964) cannot be explained on the basis of the pK_a values alone and may be due to other factors such as reagent accessibility and dynamics of the structure.

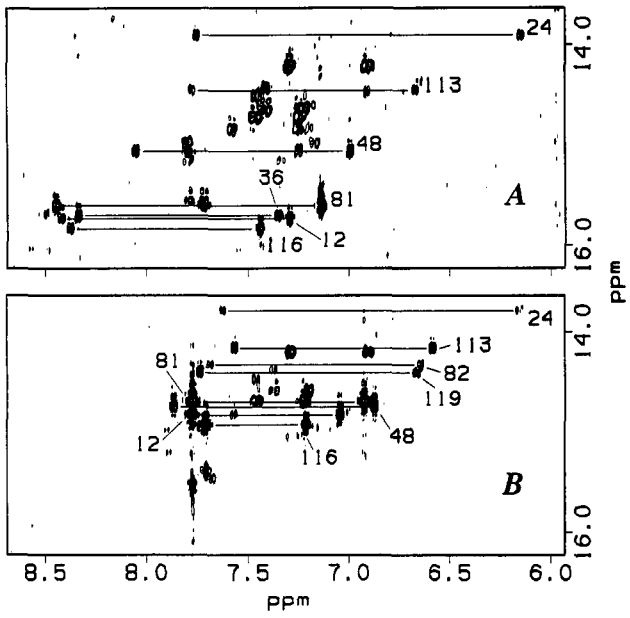

FIGURE 3: Two-quantum spectra of sperm whale metMb^2H_2O recorded at 500 MHz in ^2H_2O at 298 K at two pH* values with a total mixing time of 80 ms. Positive and negative levels are plotted without distinction. The region presents the connectivities between histidine $C^\delta H$ and $C^\epsilon H$: (A) pH* 5.7; (B) pH* 7.8. Assignments are discussed in the supplementary material.

the viscosity of the NMR samples increases noticeably, and although no sedimentation equilibrium data were collected under those conditions, the presence of higher molecular weight species is evident.

pH Titration. Myoglobin is a relatively large protein by proton NMR standards and, to complicate assignments and pK_a determinations, has a high histidine content. Signal overlap and crossover hinder chemical shift determination at practically all pH values. In several cases, line broadening occurs near the titration midpoint and renders the signals undetectable. Thus, while 1D spectra are the primary source for tracking the signals, NOESY and 2Q data must be collected along the titration to ensure that the lines being monitored are not mistaken for one another.

In metMb^2H_2O at pH* 5.7, the $C^\delta H$ signals are dispersed over 1.3 ppm and the crossover problem happens to be tractable. The strategy is therefore to ascertain the $C^\delta H$ assignments with NOESY data at a few pH values and to use 2Q spectra to correlate $C^\delta H$ and $C^\epsilon H$ signals throughout the titration. Figure 3 includes 2Q spectra for sperm whale metMb^2H_2O which demonstrate the ability to match the observable $C^\delta H$ and $C^\epsilon H$ signals; in some cases where 2Q cross peaks are not detected because of cancellation due to excessive line width, better success could be achieved with TOCSY spectra.

In apoMb, the overlap problem is severe and an extensive series of NOE spectra had to be recorded at different pH values. We used diagnostic NOE patterns to confirm the assignments throughout the titration: *36* ↔ 106 ↔ 103, 46 ↔ *48* ↔ 49, 17 ↔ *24* ↔ *119* ↔ 115 [Figure 4 in Cocco and Lecomte (1990)] and *113* ↔ 114 ↔ 24, *116* ↔ 123 (this work). An example is offered in Figure 2, where the NOE between His-24 $C^\epsilon H$ and His-119 $C^\epsilon H$ is plotted at four pH values. The nonassigned histidine resonances can be followed by spectral similarity mostly through strong NOEs from $C^\delta H$ to $C^\beta Hs$ and aliphatic groups, or by default.

Once the histidine assignments are verified, graphs of chemical shift versus pH can be constructed and pK_a values determined. Figures 4–8 contain titration data for selected

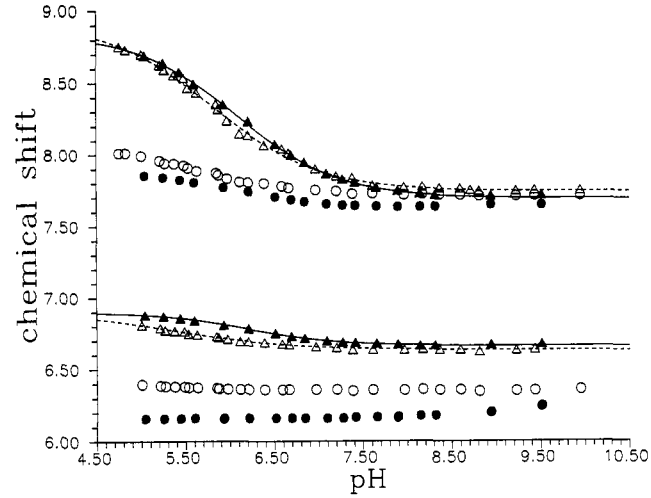

FIGURE 4: Plot of chemical shift (ppm) versus pH for His-24 and His-119 in sperm whale myoglobin: His-24 (●) and His-119 (▲) in metMb^2H_2O; His-24 (○) and His-119 (△) in apoMb. The four upper traces correspond to $C^\epsilon H$ signals while the four lower traces are for $C^\delta H$ signals. The lines through the data points were calculated by fitting to the Henderson–Hasselbalch equation. The parameters of the His-119 fit are listed in Tables III and IV. All data were collected in ^2H_2O at 298 K.

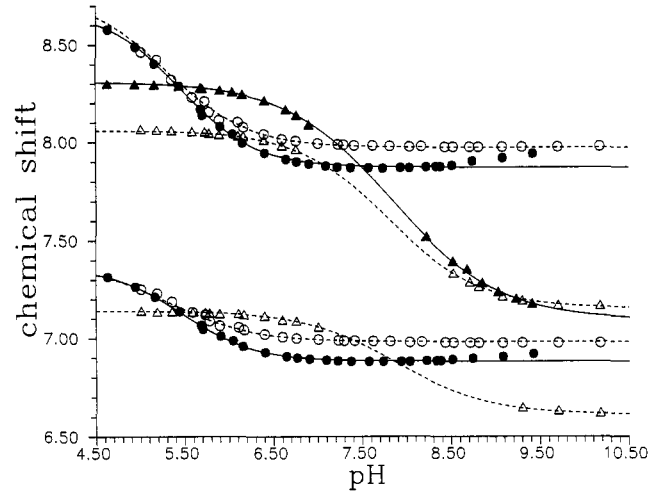

FIGURE 5: Plot of chemical shift (ppm) versus pH for His-36 and His-48 in horse myoglobin: His-36 (▲) and His-48 (●) in metMb^2H_2O; His-36 (△) and His-48 (○) in apoMb. The four upper traces are for $C^\epsilon H$ signals while the four lower traces are for $C^\delta H$ signals. The lines through the data points were calculated by fitting to the Henderson–Hasselbalch equation. The parameters of the fits are listed in Tables III and IV. All data were collected in ^2H_2O at 298 K.

residues in the holoprotein form (filled symbol) and the apoprotein form (open symbols). pK_a values and other fitting parameters are summarized in Table III (holoproteins) and Table IV (apoproteins). Additional insight can be gained by inspecting the total chemical shift excursion ($\Delta\delta = \delta_{His^+} - \delta_{His}$), which in the case of an exposed histidine residue is ca. 0.40 ppm for $C^\delta H$ and ca. 0.95 ppm for $C^\epsilon H$ (Markley, 1975). For reference, the pK_a of such an exposed residue is taken to be 6.6 (McNutt et al., 1990).

A. His-24 and His-119. Figure 4 presents chemical shift versus pH data for His-24 (circles) in sperm whale holoMb and apoMb. The behavior of $C^\delta H$ and $C^\epsilon H$ in both forms of the protein is unusual. While the chemical shift of $C^\delta H$ changes insignificantly over the pH range explored, $C^\epsilon H$ exhibits a sigmoidal response with apparent pK_a's of 6.1 (holo) and 5.5 (apo). In addition, $C^\epsilon H$ $\Delta\delta$ is only 0.4 ppm, a relatively small value suggesting that the change results from a process

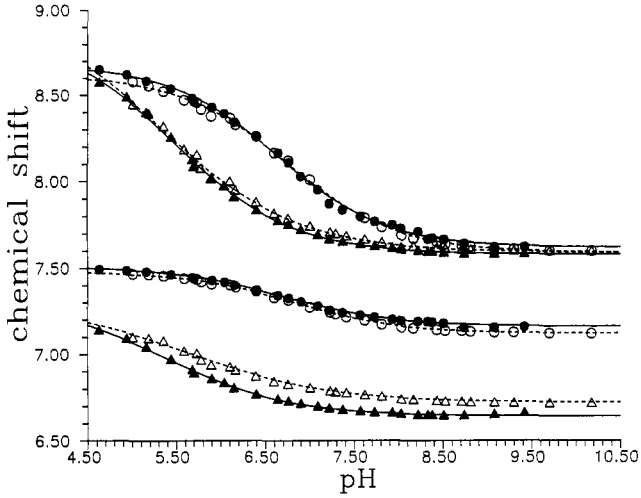

FIGURE 6: Plot of chemical shift (ppm) versus pH for His-113 and His-116 in horse myoglobin: His-113 (▲) and His-116 (●) in metMb^2H_2O; His-113 (△) and His-116 (○) in apoMb. Traces downfield of 7.5 ppm are for $C^\epsilon H$ signals; traces upfield of 7.5 ppm are for $C^\delta H$ signals. The lines through the data points were calculated by fitting to the Henderson–Hasselbalch equation. The parameters of the fits are listed in Tables III and IV. All data were collected in ^2H_2O at 298 K.

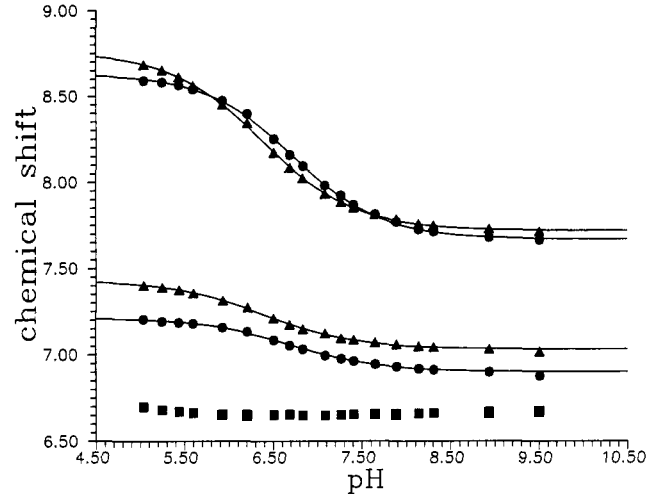

FIGURE 7: Plot of chemical shift (ppm) versus pH for other histidines in sperm whale metMb^2H_2O: His-81 (●), His-82 (■), and His-12 (▲). The two upper traces correspond to $C^\epsilon H$ signals; the three lower traces are for $C^\delta H$ signals. The lines through the data points were calculated by fitting to the Henderson–Hasselbalch equation. The parameters of the His-12 and His-81 fits are listed in Table III. All data were collected in ^2H_2O at 298 K.

Table III: pK_a Values and Titration Parameters for Histidine Residues in Metaquomyoglobin[a]

His		$\Delta\delta$[b]	δ_{His}[b]	n[c]	pK_a[c]
sw-12	δ	0.39	7.03	0.82 ± 0.03	6.39 ± 0.02
	ϵ	1.04	7.72	0.82 ± 0.02	6.38 ± 0.01
sw-24	δ/ϵ	NA	NA	NA	<4.8
sw-24	ϵ	(0.25)[d]	(7.63)	(0.87 ± 0.04)	(6.07 ± 0.03)
eq-24	δ/ϵ	NA	NA	NA	<4.8
eq-24	ϵ	(0.27)[d]	(7.68)	(0.88 ± 0.03)	(6.29 ± 0.02)
sw-36	ϵ	1.24	7.13	0.74 ± 0.02	8.18 ± 0.02[e]
eq-36	ϵ	1.22	7.09	0.72 ± 0.01	7.84 ± 0.01[e]
sw-48	δ	0.47	6.88	1.02 ± 0.05	5.52 ± 0.05[e]
	ϵ	0.77	7.87	1.00 ± 0.04	5.48 ± 0.04[e]
eq-48	δ	0.49	6.88	1.05 ± 0.04	5.46 ± 0.02[e]
	ϵ	0.81	7.87	1.03 ± 0.04	5.45 ± 0.02[e]
sw-81	δ	0.31	6.90	0.85 ± 0.03	6.69 ± 0.02
	ϵ	0.96	7.67	0.86 ± 0.02	6.73 ± 0.01
eq-81	δ	0.35	6.88	0.76 ± 0.03	6.58 ± 0.02
	ϵ	0.96	7.66	0.87 ± 0.02	6.74 ± 0.01
sw-82	δ	NA	NA	NA	<4.8
eq-82	δ	NA	NA	NA	<4.8
sw-113	δ/ϵ	NA	NA	NA	≈5.0
eq-113	δ	0.68	6.64	0.62 ± 0.02	5.37 ± 0.06[e]
	ϵ	1.30	7.58	0.65 ± 0.02	5.46 ± 0.05[e]
sw-116	δ	0.34	7.19	0.81 ± 0.02	6.59 ± 0.01
	ϵ	1.03	7.62	0.79 ± 0.02	6.60 ± 0.01
eq-116	δ	0.35	7.16	0.68 ± 0.02	6.70 ± 0.02
	ϵ	1.06	7.62	0.71 ± 0.03	6.63 ± 0.02
sw-119	δ	0.24	6.66	0.84 ± 0.04	6.20 ± 0.03[e]
	ϵ	1.16	7.69	0.75 ± 0.02	6.09 ± 0.02[e]
eq-119	δ	0.31	6.66	0.86 ± 0.03	6.39 ± 0.02[e]

[a] Values were determined at 298 K in low ionic strength solutions. NA, not available. Although raw data were obtained, the results of the fit were not considered meaningful either because the pH range accessible experimentally was not suitable to define the acidic and basic limits or because too few data points could be determined with certainty leading to extreme sensitivity to the omission of an arbitrary point. [b] $\Delta\delta = \delta_{His^+} - \delta_{His}$; δ_{His}, fitted chemical shift in the deprotonated form, δ_{His^+}, fitted chemical shift in the protonated form; all values obtained with the Henderson–Hasselbalch equation as described in Materials and Methods. Standard deviations are lower than 0.05 ppm. [c] n is the Hill coefficient, and pK_a is the apparent pK_a value provided by the fit. Standard deviations are included. The error on pK_a is estimated at ±0.1 pH unit (see Materials and Methods). [d] Values in parentheses refer to an effect attributed to the protonation of His-119 and not of His-24. [e] Although the standard deviation of the fit is within a narrow range, the curve is partially defined and the error is estimated at ±0.2 pH unit.

Table IV: pK_a Values and Titration Parameters for Histidine Residues in Apomyoglobin[a]

His		$\Delta\delta$[b]	δ_{His}[b]	n[c]	pK_a[c]
sw-24	δ/ϵ	NA	NA	NA	<4.8
sw-24	ϵ	(0.40)[d]	(7.71)	(0.68 ± 0.05)	(5.51 ± 0.08)
eq-24	δ/ϵ	NA	NA	NA	<4.8
eq-24	ϵ	(0.31)[d]	(7.78)	(0.70 ± 0.03)	(6.15 ± 0.04)
sw-36	δ	0.55	6.53	1.11 ± 0.04	8.21 ± 0.04[e]
	ϵ	0.89	7.21	1.06 ± 0.04	8.10 ± 0.04[e]
eq-36	δ	0.53	6.61	0.83 ± 0.02	7.87 ± 0.03[e]
	ϵ	0.91	7.15	0.84 ± 0.01	7.80 ± 0.01[e]
sw-48	δ	0.47	6.98	0.78 ± 0.07	5.2 ± 0.2
	ϵ	0.83	7.96	0.86 ± 0.07	5.2 ± 0.1[e]
eq-48	δ	0.41	6.98	0.91 ± 0.07	5.3 ± 0.1[e]
	ϵ	0.79	7.97	0.94 ± 0.07	5.3 ± 0.1[e]
sw-113	δ/ϵ	NA	NA	NA	<5.5
eq-113	δ/ϵ	NA	NA	NA	<5.9
sw-116	δ	0.38	7.15	0.69 ± 0.04	6.57 ± 0.03
	ϵ	1.02	7.58	0.78 ± 0.05	6.60 ± 0.04
eq-116	δ	0.36	7.12	0.72 ± 0.02	6.82 ± 0.02
	ϵ	1.03	7.59	0.70 ± 0.03	6.75 ± 0.03
sw-119	δ	0.29	6.63	0.62 ± 0.08	5.3 ± 0.3
	ϵ	1.19	7.74	0.72 ± 0.04	5.81 ± 0.05[e]
eq-119	δ	0.32	6.68	0.84 ± 0.05	6.19 ± 0.04[e]
	ϵ	1.12	7.70	0.79 ± 0.04	6.30 ± 0.03[e]
H-1-sw	δ	0.39	7.00	0.71 ± 0.04	6.41 ± 0.03
	ϵ	1.07	7.67	0.72 ± 0.04	6.39 ± 0.04
H-2-sw	δ	0.39	6.82	0.64 ± 0.05	6.48 ± 0.06[e]
	ϵ	0.93	7.62	0.77 ± 0.05	6.64 ± 0.04[e]
H-3-sw	ϵ	1.05	7.57	0.83 ± 0.05	5.73 ± 0.05[e]
H-1-eq	δ	0.33	6.82	0.68 ± 0.04	6.39 ± 0.06[e]
	ϵ	0.92	7.60	0.70 ± 0.03	6.50 ± 0.04[e]
H-2-eq	ϵ	1.05	7.57	0.77 ± 0.04	6.05 ± 0.05[e]
H-3-eq	δ	0.43	6.95	0.77 ± 0.07	5.6 ± 0.1[e]
	ϵ	1.04	7.64	0.78 ± 0.09	5.7 ± 0.1[e]
H-4-eq	δ/ϵ	NA	NA	NA	<5.7
H-5-eq	ϵ	NA	NA	NA	<4.8

[a] Values were determined at 298 K in low ionic strength solutions. [b] $\Delta\delta = \delta_{His^+} - \delta_{His}$; δ_{His}, fitted chemical shift in the deprotonated form, δ_{His^+}, fitted chemical shift in the protonated form; all values obtained with the Henderson–Hasselbalch equation as described in Materials and Methods. Standard deviations are lower than 0.05 ppm. [c] n is the Hill coefficient, and pK_a is the apparent pK_a value provided by the fit. Standard deviations are included. The error on pK_a is estimated at ±0.1 pH unit (see Materials and Methods). [d] Values in parentheses refer to an effect attributed to the protonation of His-119 and not of His-24. [e] Although the standard deviation of the fit may be within a narrow range, the curve is partially defined and the error is estimated at ±0.2 pH unit.

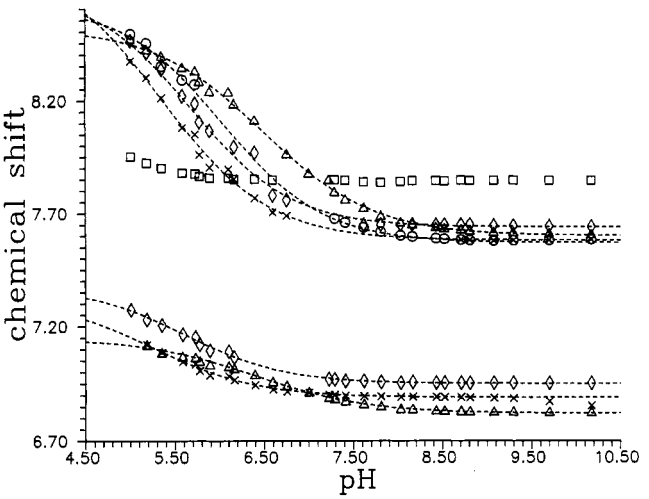

FIGURE 8: Plot of chemical shift (ppm) versus pH for other histidines in horse apoMb: H-1-eq (△), H-2-eq (○), His-3-eq (◇), His-4-eq (×), and H-5-eq (□). The five upper traces are for $C^{\epsilon}H$ signals; the three lower traces are for $C^{\delta}H$ signals. The lines through the data points were calculated by fitting to the Henderson–Hasselbalch equation. The parameters of the His-1-eq to His-4-eq fits are listed in Table IV. All data were collected in ^2H_2O at 298 K.

other than protonation of the imidazole ring. The chemical shifts indicate that His-24 remains uncharged down to the lowest pH reached in the titration. The data pertaining to sperm whale His-119 are also plotted in Figure 4 (triangles). In the holoprotein, both $C^{\delta}H$ and $C^{\epsilon}H$ titrate with a pK_a of ca. 6.2, while in the apoprotein, $C^{\epsilon}H$ yields a pK_a of 5.8 and $C^{\delta}H$ has a distinct behavior with no inflection and a lower apparent value.

In horse Mb, His-24 displays a response comparable to that in sperm whale Mb (not shown): $C^{\delta}H$ chemical shift is practically independent of pH and $C^{\epsilon}H$ describes a curve with apparent pK_a's of 6.3 (holo) and 6.2 (apo); $\Delta\delta$ is only 0.3 ppm. In the holoprotein, His-119 $C^{\epsilon}H$ is observable at pH's below ca. 5.8 and broadens beyond detection as the pH is raised above that value. However, $C^{\delta}H$ can be followed throughout the titration and yields a pK_a of 6.4. In horse apoMb, $C^{\epsilon}H$ cannot be monitored around pH 7, although $C^{\delta}H$ remains detectable throughout the titration and indicates a pK_a of 6.2. Thus, the 24–119 pair is unaffected by heme removal in horse Mb. In sperm whale Mb, the apparent pK_a's of these two residues are perturbed but, interestingly, not toward the solvent-exposed behavior. In both proteins, His-24 and -119 maintain their distinctive NOEs in the absence of the heme.

B. His-36 and His-48. Figure 5 contains the titration curves for His-36 (triangles) and His-48 (circles) in horse holo- and apoMb. In metMb^2H_2O, His-36 $C^{\epsilon}H$ gives rise to a signal which, although sharp in the protonated state, broadens through the titration and is undetectable between pH 7 and pH 8.2; the $C^{\delta}H$ signal could not be followed. In apoMb, broadening prevents detection between pH 7.0 and pH 8.5, the pH at which the signal sharpens and its characteristic NOEs reappear. On the basis of the limited number of pH data points collected for this residue, only approximate $\Delta\delta$ and pK_a values are determined. Nevertheless, it can be stated that His-36, in both the holo- and apoprotein, has the highest pK_a value of all observable titrating histidines. This is also the case in sperm whale myoglobin.

The data plotted in Figure 5 demonstrate that His-48 titrates with a low pK_a (approximately 5.5) regardless of the presence of the heme and of the animal species. Precise $\Delta\delta$ and pK_a cannot be evaluated since one of the limiting baselines is not accessible. One feature of the His-48 titration curve distinguishes apoMb from holoMb. In the holoprotein, the chemical shift of $C^{\delta}H$ and $C^{\epsilon}H$ reaches its highest field at ca. pH 8 and drifts toward lower field at more basic pH values; in the apoprotein, the chemical shift remains nearly constant above pH 8. This behavior is attributed to hemic acid dissociation (Botelho & Gurd, 1978; Carver & Bradbury, 1984), which occurs with a midpoint pH near 9 (Brunori et al., 1968; Shire et al., 1975). Thus, apart from sixth-ligand effects, His-48 and His-36 appear insensitive to heme release.

C. His-113 and His-116. Figure 6 contains the titration curves of these two G-helix histidines in horse holo- and apoMb. In horse Mb it is possible to follow the signals of His-113 (triangles) within the entire pH range. The apparent pK_a of this residue is 5.4 in the holoprotein, where the fits yield large $\Delta\delta$ values and small Hill coefficients. In the apoprotein, the lack of a suitable low-pH baseline prevents the determination of an accurate pK_a but the incomplete titration also suggests small Hill coefficient and large $\Delta\delta$ values. In sperm whale holoMb (not shown), it is difficult to monitor the broad signals of His-113 through the transition. Partial titration curves assign an apparent pK_a value of 5.0, close to that observed in horse Mb. In sperm whale apoMb, His-113 has a low pK_a which, as in horse apoMb, cannot be evaluated because the low-pH plateau is not reached before the protein unfolds and aggregates. His-116 signals (circles) are detectable throughout the titration of both holo- and apoproteins. The apparent pK_a of this residue is 6.6 and practically independent of the species and the presence of the heme.

D. Other Histidines in MetMbH_2O. Figure 7 contains the titration curves for His-12, -81, and -82 ($C^{\delta}H$ only) in sperm whale holoMb. His-12, unique to sperm whale Mb, and His-81 have pK_a's of 6.4 and 6.7, respectively. His-82 $C^{\epsilon}H$ cannot be resolved in 1D spectra while $C^{\delta}H$ gives sharp and pH-independent signals above pH* 6.0. Below that pH, $C^{\delta}H$ broadens and starts moving to lower fields at pH* 5.5. This behavior suggests a low pK_a value.

E. Other Histidines in ApoMb. The chemical shift of all remaining histidines could be monitored as a function of pH in horse apoMb. Figure 8 presents the corresponding titration curves. Only one of the unassigned residues (H-1-eq) has a pK_a close to that of an exposed imidazole side chain. Three have relatively low pK_a values, ranging between 5.5 and 6.1. One of these, H-2-eq, has multiple signals at pH* 5.7 and therefore appears to sample several conformations in the slow-exchange limit on the chemical shift time scale. The last one, H-5-eq, has a $C^{\epsilon}H$ signal whose chemical shift is independent of pH, except at low pH where a slight move to lower field is detected. Both $C^{\delta}H$ and $C^{\epsilon}H$ chemical shifts are indicative of the neutral imidazole form and therefore a histidine with low pK_a. A tentative interpretation of the pK_a values matches the nontitrating H-5-eq with His-82 and the apparently exposed H-1-eq with His-81. If these assignments are correct, then the low unassigned pK_a's pertain to the heme binding site His-64, -93, and -97. Sperm whale apoMb offers only three histidines other than those assigned above with sharp lines that can be followed throughout the titration. Two have pK_a values near 6.5 and may correspond to His-12 and -81. The third has a lower pK_a of 5.7, similar to the pK_a's proposed for the heme binding site histidines in the horse apoprotein.

F. Other Resonances. In apoMb, Trp-14 is in contact with an upfield-shifted isopropyl group [Figure 3 in Cocco and Lecomte (1990), NOEs at −0.05 ppm]. According to TOCSY pattern and comparison to the holoprotein, this group is likely to belong to Leu-76. Its chemical shift and that of a few other assigned aliphatic resonances can be followed as a function

of pH (not shown). In sperm whale apoMb, the methyl resonances of Leu-2, Val-17, Leu-40, and Leu-76 experience changes in chemical shift on the order of 0.1 ppm as the pH is lowered from 10 to 5. These shifts, which reflect the titration of nearby groups and possibly conformational changes, are not detected in horse apoMb. Below pH 5, both horse and sperm whale apoMb spectra gradually approach that of an unfolded protein (Bundi & Wüthrich, 1979). Horse spectra show no dispersion of signals below pH* 4.9, while sperm whale spectra retain some native features as low as pH* 4.5 where resolved resonances from His-24, His-36, and His-119 are recognizable. His-24 is not completely protonated at that pH.

Discussion

Assignments in MetMbH_2O. Our spectral assignments are based on 2D data sets collected in H_2O and ^2H_2O at different pH values and two temperatures in order to resolve spectral ambiguities. Our conclusions differ from the latest published study (Carver & Bradbury, 1984), and we attribute the discrepancies to the difficulty in discriminating the many histidine signals solely on the basis of 1D data. Two-dimensional spectroscopy allows us not only to pair $C^{\delta}H$ and $C^{\epsilon}H$ resonances but also to assign and follow these resonances reliably throughout the titration. Overall, our results are in complete agreement for three residues: His-12 in sperm whale Mb, His-113, and His-116 in both holoproteins.

B–GH Interface. Mb X-ray data suggest that a ring-to-ring hydrogen bond between the buried His-24 and the partially exposed His-119 stabilizes the docking of the B helix on the GH corner (Takano, 1977; Evans & Brayer, 1990). The refined neutron diffraction structure recently published by Cheng and Schoenborn (1991) and the NMR studies of Dalvit and Wright (1987) confirm the presence of the $N^{\epsilon 2}$–$N^{\epsilon 2}$ hydrogen bond in the solid state and in solution. NMR titration data also report on the state of ionization of the pair: in sperm whale MbCO, the pK_a of His-119 is 6.2 while that of His-24 is below 5 (Dalvit & Wright, 1987). The same interaction exists in metMb^2H_2O and apoMb since in those two forms of the protein His-24 and His-119 have pK_a's comparable to those in MbCO. Interresidue NOEs demonstrate that the two histidines are within hydrogen-bonding distance at pH 5.6 and remain so at least to pH 9.1. The imidazolium form of His-24 is not observed; the chemical shift response of its $C^{\epsilon}H$ has an apparent pK_a which matches well that of His-119 and is probably only a reflection of the titration of this residue (Dalvit & Wright, 1987). Protonation of His-119 is not accompanied by an alteration of NOE patterns. The B5–GH1 tertiary interaction appears to be a strong interaction which contributes to the stabilization of the apoprotein structure. In myoglobin, histidines are conserved at those positions (Dayhoff, 1978), but other pairs of residues are found in hemoglobins (Dayhoff, 1978; Bashford et al., 1987) where they may serve an equivalent structural role.

C–CD–D Region. Alkylation of sperm whale holoMb in solution at neutral pH with bromoacetate has demonstrated that His-36 is not reactive (Banaszak et al., 1963; Hugli & Gurd, 1970b). This is consistent with the relatively high pK_a (Botelho & Gurd, 1978; Carver & Bradbury, 1984; this work) presumably due in part to interaction with Glu-38 (Botelho et al., 1978; Friend & Gurd, 1979a,b; Garcia-Moreno et al., 1985). If the reaction is performed on the crystallized holoprotein at the same pH, His-36 reacts quickly (Hugli & Gurd, 1970a). Since the reagent attacks solely the imidazole state, the reactivity suggests that the pK_a is different in solution and in the crystal. The discrepancy has recently been documented; the pK_a is estimated below 5 in the solid state (Cheng & Schoenborn, 1991). We find that the high pK_a value measured for the dissolved holoprotein is maintained in the dissolved apoprotein.[2] Because the titration behaviors of His-36 are alike in the apo and holo forms, it is proposed that the environment of this residue is largely unchanged when the heme is removed and that its predominant tautomeric state at high pH [imidazole $N^{\delta}H$, Botelho et al. (1978)] is conserved. The NOE information agrees with the structural interpretation since His-36 is in dipolar contact with Phe-106. In the holoprotein His-36, Glu-38, and Phe-106 form a tight cluster (Heringa & Argos, 1991). This cluster persists under native conditions in the apoprotein, where it may indeed stabilize the structure. Electrostatic calculations performed on the holoprotein reveal that the short C helix is stabilized by intraelemental interactions among which the 36–38 ion pairing contributes the most (Friend & Gurd, 1979b; Garcia-Moreno et al., 1985). As suggested by these authors, it is possible that the proper orientation of the two side chains favors helix formation.

His-48 has $C^{\delta}H$ and $C^{\epsilon}H$ at 19 and 15 Å from the heme iron atom, respectively, and senses the transition to metMbOH. His-48 is not the only residue to present a chemical shift anomaly resulting from hemic acid dissociation. The frequency of assigned signals from nontitratable residues in metMb^2H_2O can be plotted versus pH (not shown). In both horse and sperm whale Mb, the side chains which are close to the heme (for example Phe/Tyr-151 and Leu-76) experience shifts of ca. 0.4 ppm toward lower fields between pH 7.5 and pH 9.5. Shifts of the same magnitude are not detected in the apoprotein. If we disregard these high pH effects and concentrate on the acid–base equilibrium of His-48, we can conclude that the electrostatic properties of its environment are little affected by the presence of the heme. Furthermore, NOE information describes this environment as resembling that in the holoprotein. This is consistent with the hypothesis that the turn is formed in the globin and that it may be involved in the recognition of the prosthetic group (Cocco & Lecomte, 1990).

G Helix. His-116 and -113 titration behaviors are moderately responsive to species and heme removal. His-113 has a low pK_a (Wilbur & Allerhand, 1977; Botelho & Gurd, 1978), which is attributed in the holoprotein to the proximity of Arg-31 (B12) (Gurd et al., 1980). The small Hill coefficient and large $\Delta\delta$ value obtained by fitting the data to the Henderson–Hasselbalch equation indicate that other equilibria are coupled to the protonation of the imidazole. One such process could be the protonation–deprotonation equilibrium of the nearby His-116. The pH response of His-113 in the globins is evidence that, in the absence of the heme, position B12 is folded near position G14. In this region of the structure, our pK_a and NOE data concur with amide hydrogen-exchange protection factors determined for sperm whale apoMb (Hughson et al., 1990) which support the presence of native holoprotein structure. Circular dichroism experiments on mutants at positions G9 (Hughson et al., 1991) and G11 (Hughson & Baldwin, 1989) confirm that these G-helix replacements affect the stability of the apoprotein.

E–EF–F–FG Region. In metMbH_2O, His-81 presents a titration curve characteristic of an exposed histidine. This is in agreement with crystal structure data on the EF corner (Takano, 1977; Evans & Brayer, 1990; Cheng & Schoenborn, 1991). With two-dimensional NMR methods, the resonances of the adjacent His-82 can be found. In contrast to His-81, His-82 is unaffected by pH changes above pH 6.0. According to the $C^{\delta}H$ and $C^{\epsilon}H$ chemical shifts and the downfield drift at both high and low pH's His-82 has a pK_a lower than 5. To

support this interpretation, we note that when the titration is repeated in the presence of 0.2 M sodium chloride, the chemical shift of $C^{\delta}H$ begins its move to lower field at a pH higher than without the salt. The chemical shift versus pH curve then resembles more convincingly that of a titrating imidazole (Y.-H. Kao and J. T. J. Lecomte, unpublished results). The carbon-13 NMR data collected on ferrimyoglobin by Wilbur and Allerhand (1977) identify a histidine which has a $pK_a \leq 5$ and no counterpart in the proton spectra available at the time. This unassigned residue may correspond to our His-82. A neutral His-82 is consistent with its location against the H helix, buried in the hydrophobic environment formed by Ile-75, Leu-86, Leu-137, and Phe-138, but conflicts with the neutron diffraction structure of MbCO (Cheng & Schoenborn, 1991), which shows a fully protonated His-82 in contact with Asp-141 at pH 5.7. In fact, NMR and neutron diffraction data differ for all histidines except for His-48 and -81, and the agreement for His-48 may be fortuitous as it is involved in intermolecular contacts. The discrepancies may be due in part to crystal packing effects and to the different conditions used for the diffraction study (saturated $(NH_4)_2SO_4$) and our solution studies (low ionic strength). In this respect, it is possible that the pH's of the solid-state and solution samples are significantly distinct because of salt and isotope effects even though the values are nominally 5.7 in both cases.

Although the histidines of the E–EF–F–FG elements could not be definitively assigned in the apoprotein, a plausible interpretation implies that the three low-pK_a residues are the heme-linked histidines at positions E7, F8, and FG3 which potentiometric titrations find unmasked only in apoMb (Breslow, 1962; Breslow, 1964). The depressed acidity constants are probably the consequence of local hydrophobicity and limited hydration. In this regard, we note that even His E7, which displays a propensity to move out of the heme pocket in the holoprotein (Ringe et al., 1984), would not be fully exposed to solvent in the apoprotein. At neutral pH the three heme binding site histidines would then be largely unprotonated and predominantly in the $N^{\epsilon}H$ tautomeric state (Reynolds et al., 1973; Wilbur & Allerhand, 1977). This state could readily rearrange to free the N^{ϵ} atom for coordination and help direct the heme to the correct binding site more efficiently than the imidazolium form. This contrasts with the observations made for apocytochrome b_5 in which the two axial histidines have pK_a's of 7.7 and 7.4 (Moore et al., 1991), and thus the low pK_a of the imidazole groups in the binding site does not constitute a common property of apo *b* heme proteins.

Further insight into the structure of the apoprotein E–EF–F–FG segment can be gained through nontitratable side chains such as Leu-76 (E19). Leu-76 appears positioned against Trp-14 (A12) whether the heme is present or not. The docking of the penultimate residue of the E segment on the core formed by the second tryptophan of Mb, along with the low pK_a's measured in the binding site, reinforces the proposition that the distal side of the heme pocket is formed and hints to extension to the proximal side.

Overall, we observe that removal of the heme has little influence on the majority of histidine residues not in contact with it. Prosthetic group abstraction results not only in conformational rearrangement of the polypeptide matrix but also in electrostatic redistribution ensuing upon withdrawal of the negative charges of the heme propionates and the positive charge of the iron atom. In view of these changes, the small perturbation of the pK_a's is noteworthy. It confirms that, for several of the imidazole groups, the dielectric shielding is essentially established by direct nonpolar neighbors and therefore that hydrophobic clustering assumes a dual role toward stabilizing the fold and determining its electrostatic characteristics (Garcia-Moreno et al., 1985). Thus, we find that the local structure around these residues is intact and that long-range electrostatic effects due to the heme group are unimportant. It is paradoxical that comparatively modest charge alterations such as the replacement of the iron sixth ligand by azide are transmitted through the protein (Friend & Gurd, 1979b; Gurd & Rothgeb, 1979; Friend et al., 1980; Le Tilly et al., 1991). The resolution of this issue will require a reexamination of the electrostatic properties of holoMb incorporating the correct histidine assignments and a complete analysis of the electrostatic and structural properties of apomyoglobin.

Differences between Sperm Whale Mb and Horse Mb. The parallel study of two species of myoglobin was useful in resolving spectral ambiguities and confirming assignments, in both the holo and the apo forms. The X-ray structures of sperm whale and horse $metMbH_2O$ show sizable deviations in α-carbon positions in the regions of residues 15–17 and 118–123 and at the N- and C-termini (Evans & Brayer, 1990). The patterns of NOEs involving Val-17, Leu-115, and His-119 are the same in both holoproteins, but the intensities of those NOEs vary. An interpretation of the differences can only stem from a quantitative study of the time dependence of the effects and is beyond the scope of this work. However, pK_a data do provide some information.

His-119 is located in the variable region of the structure. Position 118 is occupied by either a Lys (horse) or an Arg (sperm whale) and may be responsible for the small deviation in pK_a observed in the two proteins. His-24, the hydrogen-bond partner of His-119, exhibits an apparent pK_a which is thought to reflect the titration of His-119 and is also slightly species-dependent. Removal of the heme from the horse holoprotein yields an unchanged 24–119 pair; in contrast, removal of the heme from the sperm whale holoprotein lowers the pK_a of His-119 by ca. 0.3 pH unit. It is possible that the additional interactions imposed by the heme force the two holoprotein structures to resemble each other whereas the release of these constraints allows the apoproteins to relax to distinct local conformations. The occurrence of different apoprotein structures which are readjusted to a common fold through heme binding has been observed for the two subunits of hemoglobin (Yip et al., 1972). It is interesting and perhaps significant that a lower His-119 pK_a is observed in sperm whale apoMb, the apoprotein which retains nonstatistical spectral features at lower pH.

In addition to pK_a's, other NMR indicators point to unique features of each apoprotein. For example, Leu-76 and Val-17 are sensitive to pH in sperm whale but not in horse apoMb. These residues are both in the ring current of Trp-14 and may reflect slightly different conformations or conformational fluctuations around the indole group. In the CD corner, the pattern of NOEs due to contact between Met-55 $C^{\epsilon}H_3$ and the phenyl ring of Phe-33 suggests a local alteration of conformation. In the same region of the structure, Phe-43 (CD1) displays broad line widths indicative of conformational exchange. Alone, these manifestations do not support a global structural difference but indicate that specific regions do respond to variations in primary structure.

Structure of Apomyoglobin. The clusters identified previously (Cocco & Lecomte, 1990) are stable at least between pH* 5 and pH* 9.0 (with the reservation that the NOEs

between His-36 and Phe-106 are not resolved above pH* 6.8). They suggest that the A, B, C, G, and H helices and CD corner are partially formed. In the course of the studies described above, we found in sperm whale apoMb five amide protons which exchange slowly with solvent deuterons at pH* 5.7 and are detected within 1 day after dissolving in ^2H_2O. At least one of these occurs in the A helix (NOE to Trp-14) and one in the G helix (NOE to Leu-115). The amide hydrogen-exchange kinetics of sperm whale apoMb have been studied indirectly through rapid quenching of the reaction with heme addition (Hughson et al., 1990). The results of these experiments indicate that amide protons are protected in each of the elements which form helices in the holoprotein except the D and the F helices. The retardation has been attributed to the presence of secondary structure detected by CD measurements. The persistence of backbone NH signals that we observe in the absence of the heme may also be a manifestation of secondary structure underlying the tertiary interactions evidenced by the clusters.

Apomyoglobin is known to form a stable acid-unfolding intermediate at pH 4.2 and 3 °C (Hughson et al., 1990). Circular dichroism data reveal that 35% of the residues are involved in helical conformation. The results of systematic mutational studies designed to characterize the nature of the interactions stabilizing the intermediate support the hypothesis that it is a molten globule (Hughson et al., 1991). The population of this intermediate has not been evaluated at room temperature. The NMR spectrum of the sperm whale globin has been reported at pH 4.8 and 27 °C, where native features were observed (Griko et al., 1988). At pH* 4.5 and 25 °C in ^2H_2O, weak signals from His-24, His-36, and His-119 are resolved which can be attributed to a small population of folded molecules. The spectrum appears as a superimposition of a statistical coil spectrum and a partially folded spectrum. It does not resemble that of the compact species with secondary structure (A state) described by Baum and co-workers (1989) for α-lactalbumin. Below pH 5 and at the concentration of 1 mM used for the NMR experiments, a noticeable increase in solution viscosity accompanies a loss of structural features and is a strong indicator of aggregation. It is likely that this phenomenon interferes with the detection of compact species by driving the conformational equilibria to the unfolded form.

The proton NMR spectrum of apoMb is not amenable to a complete structural study by conventional means. Yet, it was possible to extract information on the properties of the molecule by analyzing the response of histidines to pH changes. Myoglobin contains a considerable number of these residues which in the holoprotein have pK_a's spread over several units, a fact demonstrating their sensitivity to local environment and validating their use as probes. Our interpretation of apomyoglobin NMR spectra is based on the hypothesis that structural features, if present, are likely to resemble those of the holoprotein. In several cases, this is amply confirmed by NOE data. In others, the evidence is weaker and needs to be strengthened, for example, by the use of heteronuclear methods. It is interesting that in horse apoMb, the protein which lends itself to a more complete study, the environment of six, perhaps eight, histidines generates the same electrostatic properties as in the holoprotein. Thus, although the details of the geometry and dynamics are not conserved around each of those residues, the structure and compactness result in the same apparent acidity constants as in the holoprotein. When the pK_a information is combined with that on the clusters, the most severe structural consequences of heme abstraction appear to be confined to the proximal region of the binding site and the cores likely to be responsible for the cooperative behavior of the apoprotein (Griko et al., 1988) appear organized as in the holoprotein.

Acknowledgments

Numerous discussions with Dr. Bertrand Garcia-Moreno were most motivating and helpful to initiate and complete this work. We thank Dr. Gary Brayer for providing the X-ray coordinates of horse metMbH_2O, Doug Barrick for advice, comments, and communication of results prior to publication, and Dr. C. Robert Matthews for comments on the manuscript.

Supplementary Material Available

Description of the spectral assignments in horse and sperm whale metMbH_2O, a figure showing the TOCSY and NOESY cross peaks in the amide–aromatic region of horse metMbH_2O at pH 5.7 and 298 K, and a figure showing the NOESY connectivities from the aromatic region to the aliphatic region between 1.2 and −0.8 ppm (4 pages). Ordering information is given on any current masthead page.

Registry No. His, 71-00-1.

References

Abrash, H. I. (1970) *C. R. Trav. Lab. Carlsberg 37*, 129–144.
Anderson, S. R., Brunori, M., & Weber, G. (1970) *Biochemistry 9*, 4723–4729.
Anfinsen, C. B., & Sheraga, H. A. (1975) *Adv. Prot. Chem. 29*, 205–300.
Baldwin, R. L. (1975) *Annu. Rev. Biochem. 44*, 453–475.
Banaszak, L. J., Andrews, P. A., Burgner, J. W., Eylar, E. H., & Gurd, F. R. N. (1963) *J. Biol. Chem. 238*, 3307–3314.
Bashford, D., Chothia, C., & Lesk, A. M. (1987) *J. Mol. Biol. 196*, 199–216.
Baum, J., Dobson, C. M., Evans, P. A., & Hanley, C. (1989) *Biochemistry 28*, 7–13.
Bismuto, E., Colonna, G., & Irace, G. (1983) *Biochemistry 22*, 4165–4169.
Bodenhausen, G., Kogler, H., & Ernst, R. R. (1984) *J. Magn. Reson. 58*, 370–388.
Botelho, L. H., & Gurd, F. R. N. (1978) *Biochemistry 17*, 5188–5196.
Botelho, L. H., Friend, S. H., Matthew, J. B., Lehman, L. D., Hanania, G. I. H., & Gurd, F. R. N. (1978) *Biochemistry 17*, 5197–5205.
Braunschweiler, L., & Ernst, R. R. (1983) *J. Magn. Reson. 53*, 521–528.
Braunschweiler, L., Bodenhausen, G., & Ernst, R. R. (1983) *Mol. Phys. 48*, 535–560.
Breslow, E. (1962) *J. Biol. Chem. 237*, PC3308–PC3311.
Breslow, E. (1964) *J. Biol. Chem. 239*, 486–496.
Breslow, E., Beychok, S., Hardman, K. D., & Gurd, F. R. N. (1965) *J. Biol. Chem. 240*, 304–309.
Brooks, C. L., III (1992) *J. Mol. Biol.* (in press).
Brunori, M., Amiconi, G., Antonini, E., Wyman, J., Zito, R., & Rossi Fanelli, A. (1968) *Biochim. Biophys. Acta 154*, 315–322.
Bundi, A., & Wüthrich, K. (1979) *Biopolymers 18*, 285–297.
Carver, J. A., & Bradbury, J. H. (1984) *Biochemistry 23*, 4890–4905.
Chan, H. S., & Dill, K. A. (1991) *Annu. Rev. Biophys. Biophys. Chem. 20*, 447–490.
Cheng, X., & Schoenborn, B. P. (1991) *J. Mol. Biol. 220*, 381–399.
Cocco, M. J., & Lecomte, J. T. J. (1990) *Biochemistry 29*, 11067–11072.

Crumpton, M. J., & Polson, A. (1965) *J. Mol. Biol. 11*, 722–729.
Dalvit, C., & Wright, P. E. (1987) *J. Mol. Biol. 194*, 313–327.
Davis, D. G. (1989) *J. Magn. Reson. 81*, 603–607.
Dayhoff, M. O. (1978) *Atlas of Protein Sequence and Structure*, Vol. 5, Suppl. 3, National Biomedical Research Foundation, Washington, DC.
Drobny, G., Pines, A., Sinton, S., Weitekamp, D. P., & Wemmer, D. (1979) *Symp. Faraday Soc. 13*, 49–55.
Evans, S. V., & Brayer, G. D. (1990) *J. Mol. Biol. 213*, 885–897.
Feng, Y., & Sligar, S. G. (1991) *Biochemistry 30*, 10150–10155.
Feng, Y., Wand, J., & Sligar, S. G. (1991) *Biochemistry 30*, 7711–7717.
Friend, S. H., & Gurd, F. R. N. (1979a) *Biochemistry 18*, 4612–4619.
Friend, S. H., & Gurd, F. R. N. (1979b) *Biochemistry 18*, 4620–4630.
Friend, S. H., March, K. L., Hanania, G. I. H., & Gurd, F. R. N. (1980) *Biochemistry 19*, 3039–3047.
Garcia-Moreno E., B., Chen, L. X., March, K. L., Gurd, R. S., & Gurd, F. R. N. (1985) *J. Biol. Chem. 260*, 14070–14082.
Goto, Y., & Fink, A. L. (1990) *J. Mol. Biol. 214*, 803–805.
Goto, Y., Calciano, L. J., & Fink, A. L. (1990) *Proc. Natl. Acad. Sci. U.S.A. 87*, 573–577.
Griko, Y. V., Privalov, P. L., Venyaminov, S. Y., & Kutyshenko, V. P. (1988) *J. Mol. Biol. 202*, 127–138.
Gurd, F. R. N., & Rothgeb, T. M. (1979) *Adv. Protein Chem. 33*, 73–163.
Gurd, F. R. N., Friend, S. H., Rothgeb, T. M., Gurd, R. S., & Scouloudi, H. (1980) *Biophys. J. 10*, 65–75.
Harrison, S. C., & Blout, E. R. (1965) *J. Biol. Chem. 240*, 299–303.
Heringa, J., & Argos, P. (1991) *J. Mol. Biol. 220*, 151–171.
Hughson, F. M., & Baldwin, R. L. (1989) *Biochemistry 28*, 4415–4422.
Hughson, F. M., Wright, P. E., & Baldwin, R. L. (1990) *Science 249*, 1544–1548.
Hughson, F. M., Barrick, D., & Baldwin, R. L. (1991) *Biochemistry 30*, 4113–4118.
Hugli, T. E., & Gurd, F. R. N. (1970a) *J. Biol. Chem. 245*, 1930–1938.
Hugli, T. E., & Gurd, F. R. N. (1970b) *J. Biol. Chem. 245*, 1939–1946.
Irace, G., Bismuto, E., Savy, F., & Colonna, G. (1986) *Arch. Biochem. Biophys. 244*, 459–469.
Katz, S., Crissman, J. K., & Beall, J. A. (1973) *J. Biol. Chem. 248*, 4840–4845.
Kim, P. S., & Baldwin, R. L. (1982) *Annu. Rev. Biochem. 51*, 459–489.
Kumar, A., Ernst, R. R., & Wüthrich, K. (1980) *Biochem. Biophys. Res. Commun. 95*, 1–6.
Lecomte, J. T. J., & Cocco, M. J. (1990) *Biochemistry 29*, 11057–11067.
Lecomte, J. T. J., & Moore, C. D. (1991) *J. Am. Chem. Soc. 113*, 9663–9665.
Le Tilly, V., Sire, O., Alpert, B., Chinsky, L., & Turpin, P.-Y. (1991) *Biochemistry 30*, 7248–7253.
Levinthal, C. (1968) *J. Chim. Phys. 65*, 44–45.
Marion, D., & Wüthrich, K. (1983) *Biochem. Biophys. Res. Commun. 113*, 967–974.
Markley, J. (1975) *Acc. Chem. Res. 8*, 70–80.
McNutt, M., Mullins, L. S., Raushel, F. M., & Pace, C. N. (1990) *Biochemistry 29*, 7572–7576.
Moore, C. D., & Lecomte, J. T. J. (1990) *Biochemistry 29*, 1984–1989.
Moore, C. D., Al-Misky, O. N., & Lecomte, J. T. J. (1991) *Biochemistry 30*, 8357–8365.
Otting, G., Widmer, H., Wagner, G., & Wüthrich, K. (1986) *J. Magn. Reson. 66*, 187–193.
Rance, M. (1987) *J. Magn. Reson. 74*, 557–564.
Rance, M., & Wright, P. E. (1986) *J. Magn. Reson. 66*, 372–378.
Rance, M., Sørensen, O. W., Bodenhausen, G., Wagner, G., Ernst, R. R., & Wüthrich, K. (1983) *Biochem. Biophys. Res. Commun. 117*, 479–485.
Reynolds, W. F., Peat, I. R., Freedman, M. H., & Lyerla, J. R. (1973) *J. Am. Chem. Soc. 95*, 328–331.
Ringe, D., Petsko, G. A., Kerr, D., & Ortiz de Montellano, P. R. (1984) *Biochemistry 23*, 2–4.
Rumen, N. M., & Apella, E. (1962) *Arch. Biochem. Biophys. 97*, 128–133.
Shaka, A. J., Lee, C., & Pines, A. (1988) *J. Magn. Reson. 77*, 274–293.
Shire, S. J., Hanania, G. I. H., & Gurd, F. R. N. (1975) *Biochemistry 14*, 1352–1358.
Stigter, D., Alonso, D. O., & Dill, K. A. (1991) *Proc. Natl. Acad. Sci. U.S.A. 88*, 4176–4180.
Takano, T. (1977) *J. Mol. Biol. 110*, 537–568.
Wilbur, D. J., & Allerhand, A. (1977) *J. Biol. Chem. 252*, 4968–4975.
Yip, Y. K., Waks, M., & Beychok, S. (1972) *J. Biol. Chem. 247*, 7237–7244.